THE INVESTIGATION OF VIBRATION OF LINAC AT KEK

Kazuyoshi Katayama , Yoshinori Takahashi , Tamio Imazawa and Nobuyoshi Murai
TAKENAKA Corporation, Technical Research Laboratory, Osaka, Japan
Tsunehiro Tamaki
TAKENAKA Corporation, Office of Plant engineering, Tokyo, Japan

1. INTRODUCTION

This report describes the results of an investigation of vibration of Linac located at KEK. The objective of the investigation was to understand the dynamic characteristics of the installation floor and components and thus to get the data for accelerator alignment.

2. OUTLINE OF THE INVESTIGATION

We investigated the vibration of Linac at KEK on December 1, 1989 and January 23, 1990, and measured the vibration of the installation floor and components and the relative vibration of accelerator tube and Q magnet. The measurement was conducted in the following four conditions. the measurement points and measurement directions are shown in Fig. 2.1 and Table 2.1.

(a) Shutdown state of Linac
(b) Transient period from shutdown state to steady operational state of Linac
(c) Steady operational state of Linac
(d) Shutdown state of air conditioning equipment and cooling water system (Total shutdown)

Fig. 2.2 is a block diagram of the measurement and analysis. The measurement was conducted using the two kinds of transducer. The low frequency range (30 Hz or below) was measured using a servo accelerometer and the high frequency range was measured using a piezo-electric transducer. The sensors were fixed directly to the target component or to a plate fastened to it.

After the measured signals were decomposed into frequency domain using Fourier analyzer, the displacement was calculated based on an assumed sine wave response. Acceleration was converted into displacement using the following equation (1).

$$F_D(\mathrm{nm}) = F_A(\mathrm{gal})/\omega^2 \times 10^7 \qquad \cdots\cdots\cdots\cdot \quad (1)$$

where F_A : Acceleration amplitude F_D : Displacement amplitude
ω : Angular frequency(rad/sec) = 2 x π x f (Hz)

In the measurement, we employed a bandpass filter, 0-50Hz, 5-100Hz, 50-500Hz and 0-5kHz, and sought to improve the SN ratio by determining the amplifier gain. We also sought to improve the accuracy of spectrum and transfer function analysis by using the averaging or cross-power method. Fourier analysis was applied to analyze the seven bandwidths - 25Hz, 50Hz, 100Hz, 250Hz, 500Hz, 1kHz and 2.5kHz - as well as the 1/256th of the bandwidths corresponding to the frequency resolution.

3. RESULTS AND DISCUSSION

3.1 Steady operational state and shutdown state of Linac

Figs. 3.1-3.3 show the acceleration waveforms and' power spectra when a direct force exitation was added to the stand. In Figs. 3.1 and 3.2, a fairly large external force was artificially given in the X direction. Fig. 3.3 shows the results when a external force was continuously added to the components on the stand using a small plastic hammer. Figs.

3.4-3.7 show the acceleration level waveform and displacement waveform of the floor and stand as well as the displacement spectra of the components in a steady operational state and in a shutdown state. Fig. 3.8 shows the acceleration level waveform of the floor and stand using a pulse magnet in the operational and shutdown states. From these measurement results, we conclude as follows:

1) Judging by the power spectra when a direct force was added, we concluded that the primary natural frequency in the X direction is about 15 Hz while the principal dynamic characteristics of the components on the stand range 500 Hz to 2 kHz.
2) The waveform in Figs. 3.4 and 3.5 suggest that when Linac is operated, the acceleration level of the stand increases about three times (10 dB) compared to shutdown state. However, no remarkable change in the displacement waveform was found. The increase in the acceleration level was so sharp, but the influence in amplitude due to transient response may be small.
3) When observing the displacement spectra in Figs. 3.6 and 3.7 while taking into consideration the characteristics cited in 1), no difference in displacement was found in the area dominating a floor vibration frequency of 5 Hz or less. We suppose that the floor and components are unified in order to display the same behavior. In the frequency area around 15 Hz which dominates the dynamic characteristics in the horizontal direction of the stand, the difference in amplitude between the floor and components is conspicuous. It should also be noted that in high frequencies, the amplitude of the components fluctuates from one to another, exhibiting individual characteristics.
4) As is obvious from viewing the displacement spectra, the effect attributable to the operation of Linac is conspicuous, particularly in the frequency range of 500 Hz or higher.
5) Fig. 3.8 suggests that the acceleration level decreases abruptly when the pulse magnet stops working.
6) As a result of observations 1)-5) above, we conclude that the change in vibration amplitude from the shutdown state to the steady state arises from operation of the pulse magnet or other equipments which vibrates upper part of the stand.

3.2 Relative vibration of Q magnet and accelerator tube

Fig. 3.9 shows the relative displacement spectra of the Q magnet and the accelerator tube in the steady operational state of Linac.

The relative displacement was calculated as follows:

$$\Delta F = |F_K \times \cos(\omega t) - F_Q \times \cos(\omega t + \phi)| \quad \cdots\cdots\cdots\cdots \quad (2)$$

where ω : Angular frequency ϕ : Phase lag in transfer function

F_K, F_Q : Displacement amplitudes of the accelerator tube and Q magnet

AF : Relative displacement

Fig. 3.10 shows the vibration patterns in which the observed relative displacement differs depending on the measurement condition and the frequency area. We regard it as appropriate to take the floor and components as a unit in the frequency range of 5 Hz or less which dominates the floor vibration, and thus the relative displacement in the figure is able to plot the range with a 5 Hz or higher frequency. When utilizing the relative displacement amplitude of the accelerator tube and Q magnet, shown in Fig. 3.9, the three vibration patterns shown in Fig. 3.10 should be taken into account.

The three vibration patterns are : (a) the pattern which the floor vibration dominate and components behave as one, (b) the pattern in which a difference between the heights of the measuring points (including the apparent relative displacement) is observed due to dynamic characteristics of the stand, and (c) the pattern in which the relative displacement is appropriately evaluated using the individual dynamic characteristics.

The frequency which forms the boundary between the vibration patterns in (a) and that in (b) was found to be around 5 Hz as stated before. But it is difficult to define the frequency which forms the boundary between the vibration patterns (b) and (c).

We have concluded that the effect of the apparent relative displacement becomes smaller as the frequency increases beyond 15 Hz.

3.3 Operational state and shutdown state of air conditioning equipment and cooling water system

Figs. 3.11-3.16 compare the displacement spectra of the floor and components in the operational state and in the shutdown state of the air conditioning equipment and cooling water system. Cooling water systems A, B and C means those for accelerator tube, Q magnet and pulse magnet, respectively. Because the cooling water system A was not completely bled of the air, the force generated by circulation of the cooling water is deemed different from the condition in the steady operational state. From these measurement results, the following points have been inferred.

1) When the displacement spectra of the floor and components in the operational state of the air conditioning equipment and cooling water system (Fig. 3.11) are compared with those during total shutdown (Fig. 3.12), displacement of each components in the range higher than 5 Hz are lower during shutdown.
2) Similarly, when the displacement spectra in the steady operational state (Fig. 3.6) are compared with those during shutdown (Fig. 3.12), all frequency constituents of components higher than 5 Hz are lower during shutdown.
3) When the displacement spectra in the operational state of the air conditioning equipment and cooling water system (Fig. 3.11) are compared with those when only cooling water system A (Fig. 3.13) is operating, the spectra in both concur almost completely. We have concluded that the vibration of the components observed are attributable to the cooling water circulating in system A.
4) When the displacement spectra during complete shutdown (shown in Fig. 3.12) are compared with those when only the air conditioning equipment is in operation (Fig. 3.16), some effects on displacement are found in the 20-100 Hz frequency area. However, the effect is smaller than that when cooling water is circulating.
5) Considering items l)-4) above, the vibration currently measured in components can be attributed to the internal vibration of the cooling water circulating through components rather than to floor vibration caused by the operation of the air conditioning equipment.

4. CONCLUSION

Our investigation has allowed us to understand the dynamic characteristics of the floor and components as well as the frequency ranges affected by changes in operating conditions. We have clarified that the currently measured vibration of components is caused by internal vibration of cooling water circulating through the components and of the pulse magnet rather than by the floor vibration caused by operation of the air conditioning equipment.

Table 2.1 Measurement direction

Components	Floor			Stand			Q magnet			Accelerator tube		
Direction	X	Y	Z	X	Y	Z	X	Y	Z	X	Y	Z
Meas. or not	○	○	×	○	○	×	○	○	×	○	○	×

○:Measured direction ×:Direction not measured

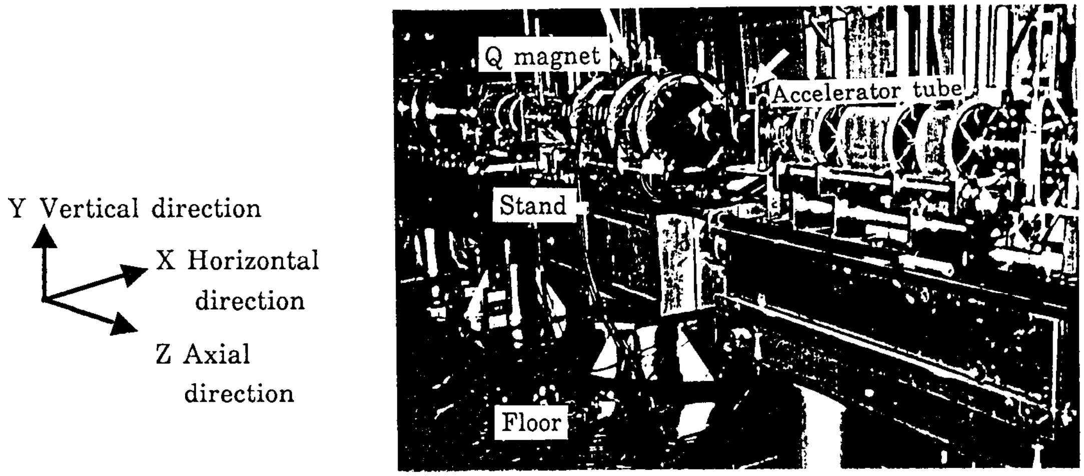

Fig. 2.1 Measurement points

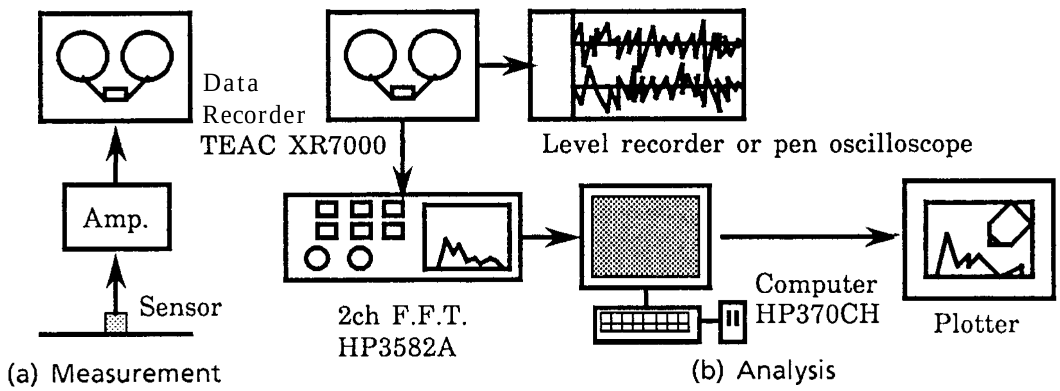

Fig. 2.2 Block diagram of measurement and analysis

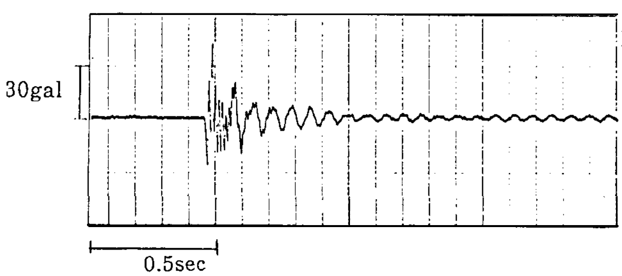

Fig. 3.1 Acceleration waveform when external force added
(In the X direction of the stand)

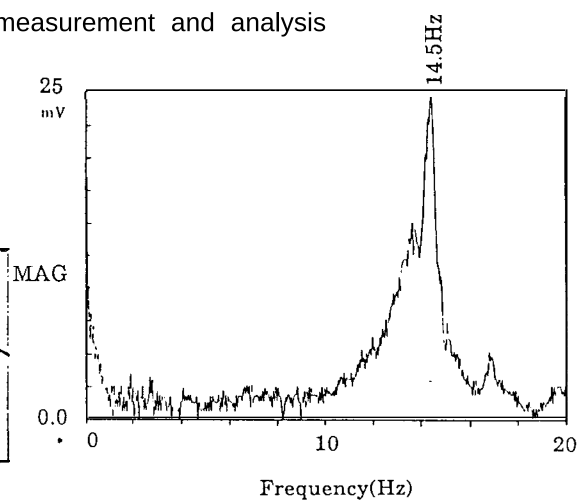

Fig. 3.2 Power spectrum when external force added in the low frequency range and X direction of the stand

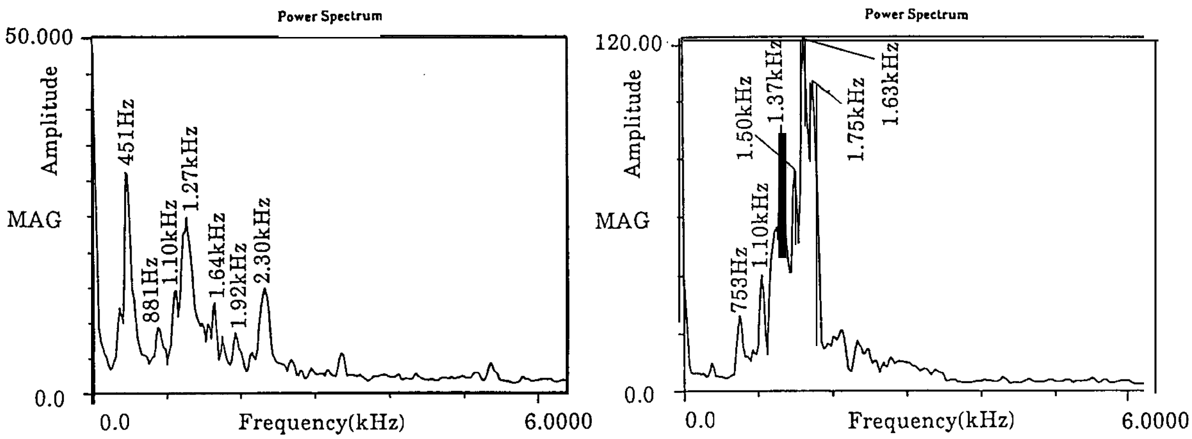

(a) X direction of the stand (b) Y direction of the stand

Fig. 3.3 Power spectrum when shock vibration administered in high-freq. area

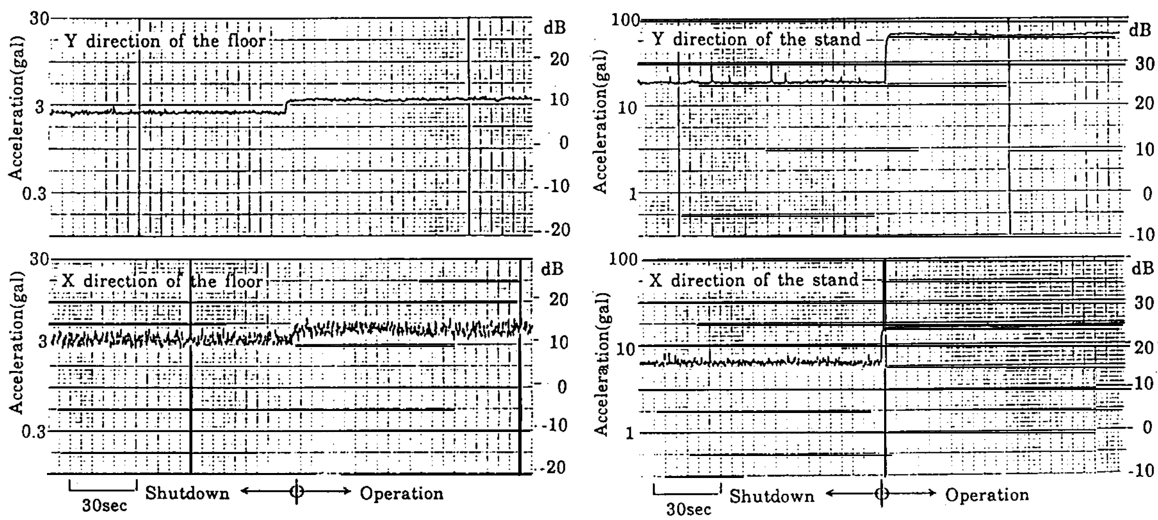

(a) On the floor (b) On the stand

Fig. 3.4 Acceleration level waveforms of the floor and the stand in the steady operational state and the shutdown state of LINAC

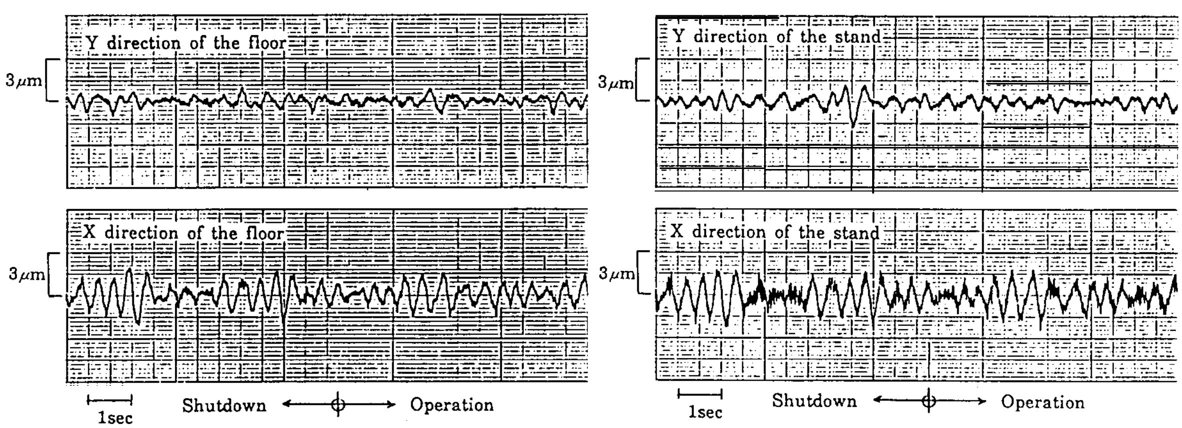

(a) On the floor (b) On the stand

Fig. 3.5 Displacement waveforms of the floor and the stand in the steady operational state and the shutdown state of LINAC

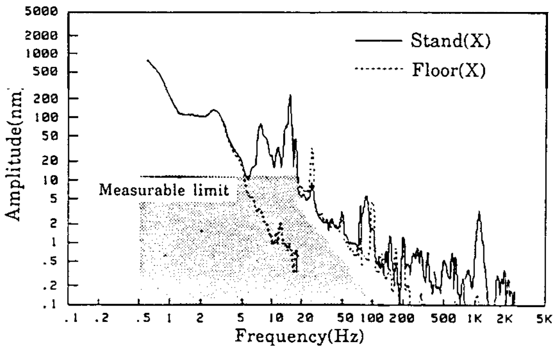

(a) X direction of Floor and Stand

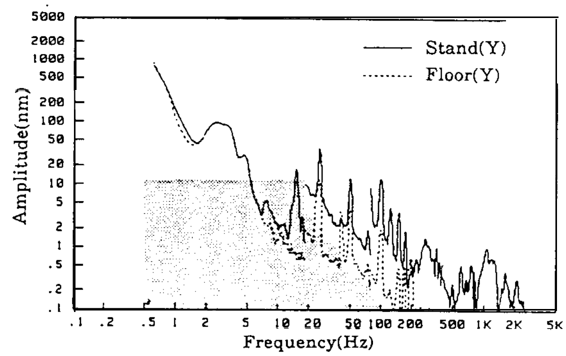

(c) Y direction of Floor and Stand

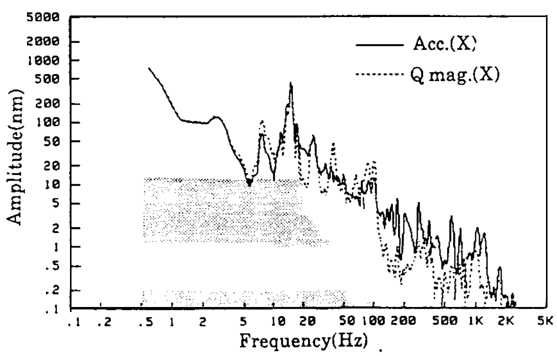

(b) X direction of Q mag. and Acc.

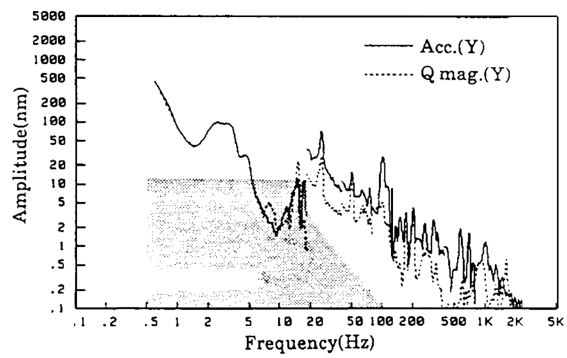

(d) Y direction of Q mag. and Acc.

Fig. 3.6 Displacement spectra in the steady operational state of LINAC

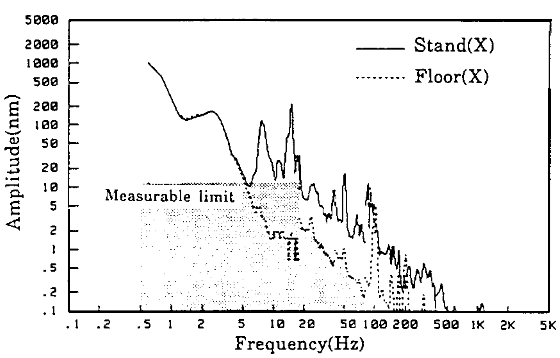

(a) X direction of Floor and Stand

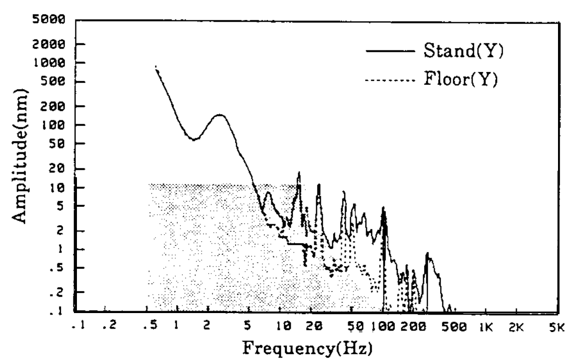

(c) Y direction of Floor and Stand

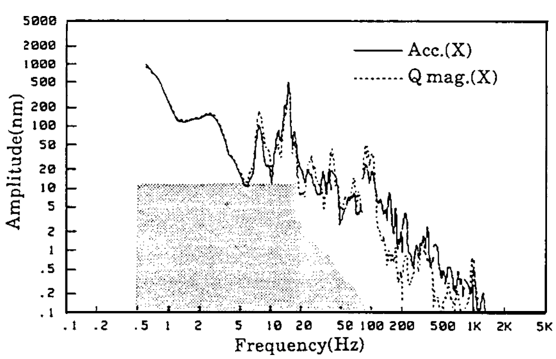

(b) X direction of Q mag. and Acc.

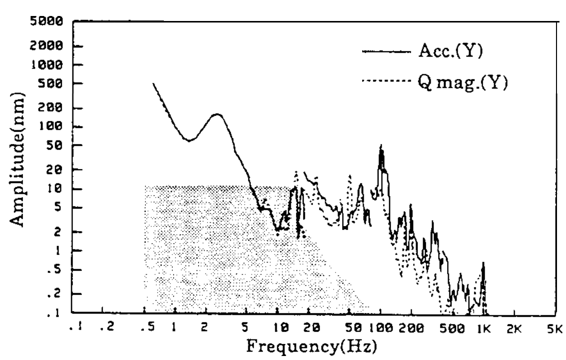

(d) Y direction of Q mag. and Acc.

Fig. 3.7 Displacement spectra in the shutdown state of LINAC

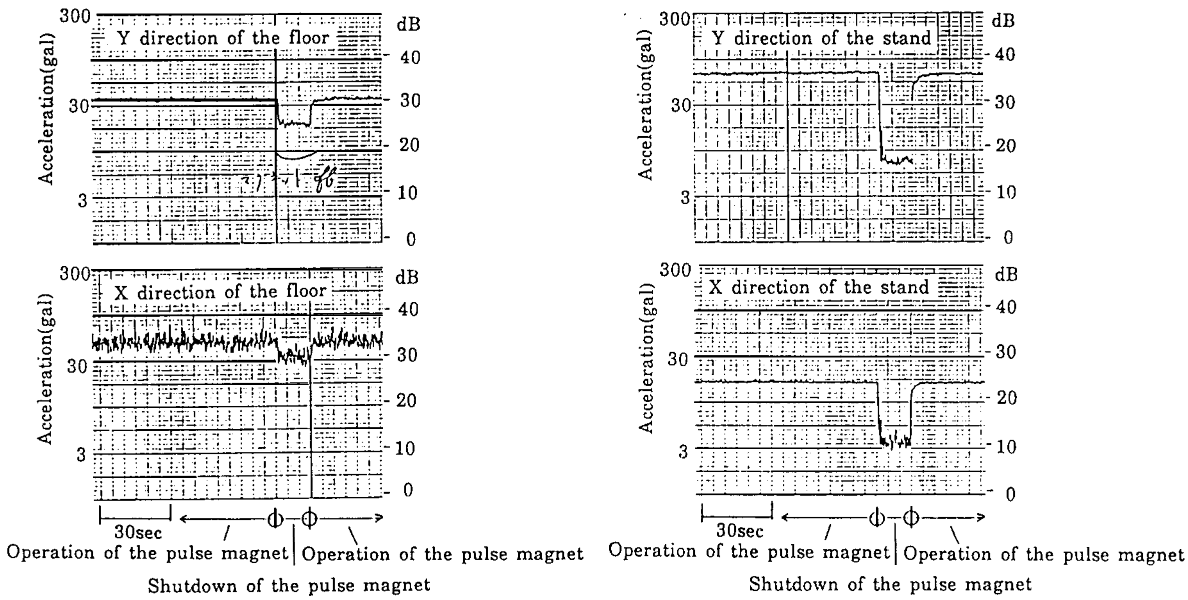

Fig. 3.8 Acceleration level waveforms of the floor and the stand in the operational state and shutdown state of the pulse magnet

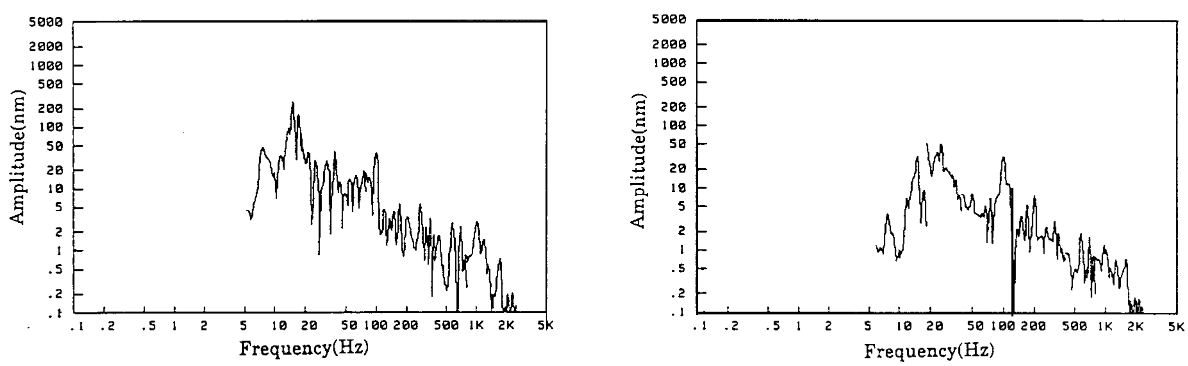

(a) X direction

(b) Y direction

Fig. 3.9 Relative displacement spectra of the Q magnet and accelerator when LINAC is in the steady operational state

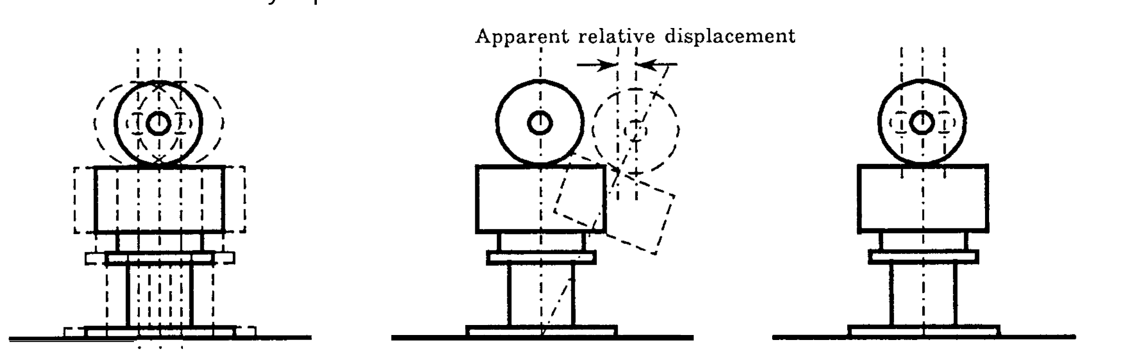

(a) Area the floor vibration chracteristics dominate

(b) Area the stand vibration chracteristics dominate

(c) Area the individual vibration chracteristics dominate

Fig. 3.10 Three vibration patterns which generate relative displacement

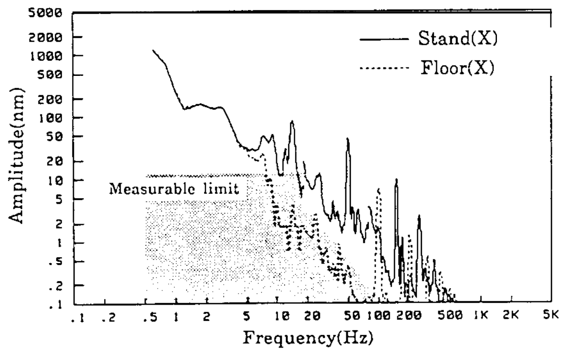

(a) X direction of Floor and Stand

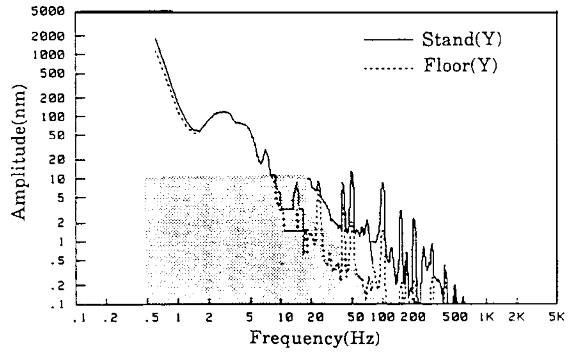

(c) Y direction of Floor and Stand

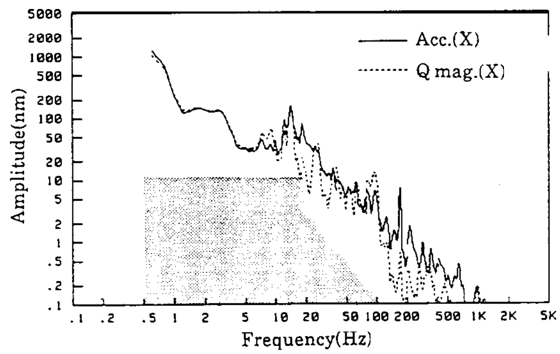

(b) X direction of Q mag. and Acc.

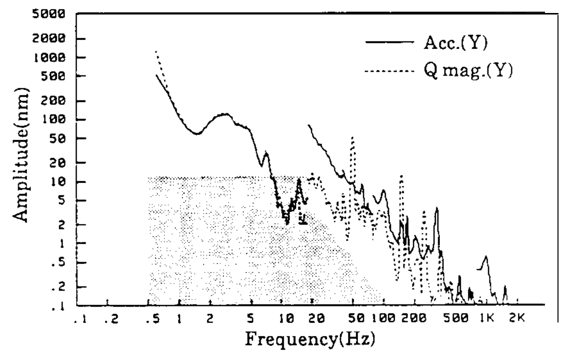

(d) Y direction of Q mag. and Acc.

Fig. 3.11 Displacement spectra in the operational state of the air conditioning equipment and cooling water system

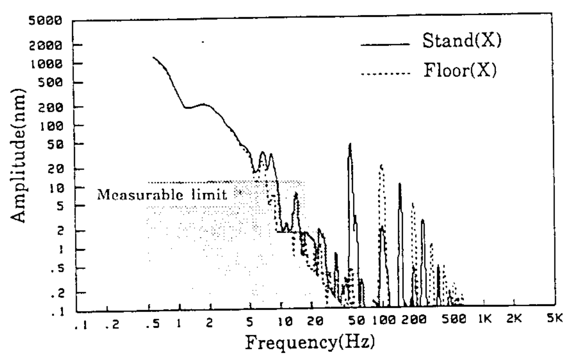

(a) X direction of Floor and Stand

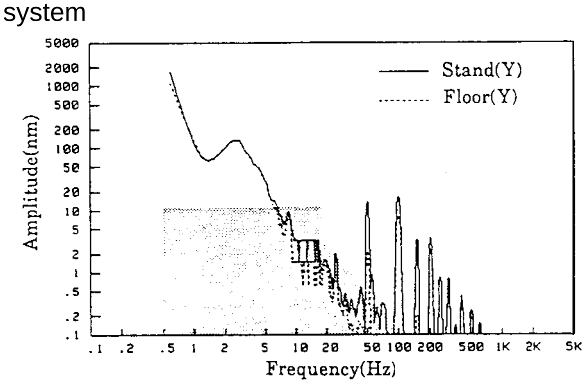

(c) Y direction of Floor and Stand

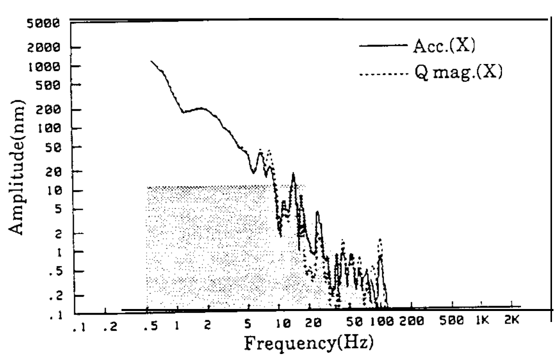

(b) X direction of Q mag. and Acc.

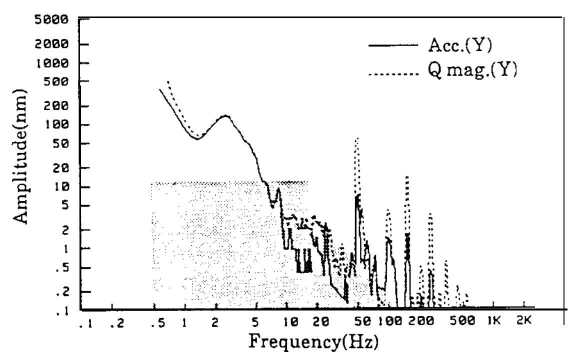

(d) Y direction of Q mag. and Acc.

Fig. 3.12 Displacement spectra during total shutdown

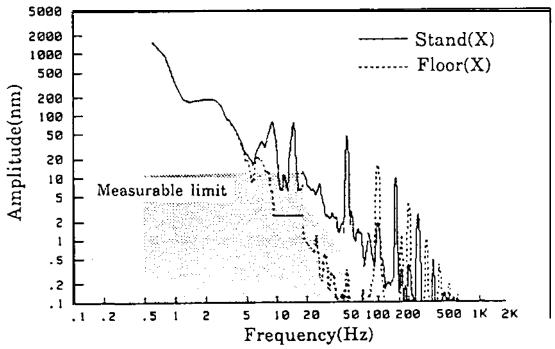

(a) X direction of Floor and Stand

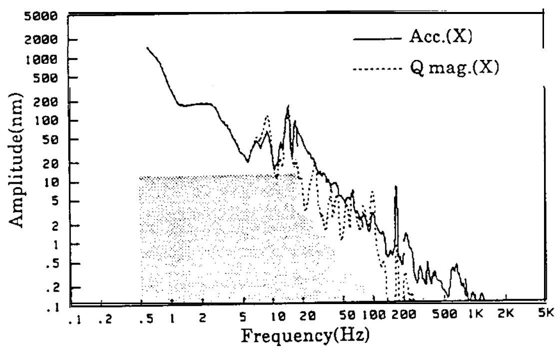

(b) X direction of Q mag. and Acc.

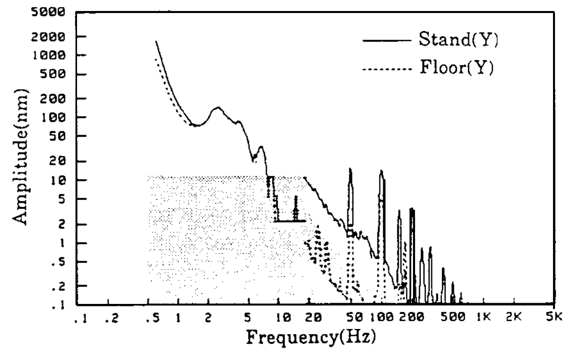

(c) Y direction of Floor and Stand

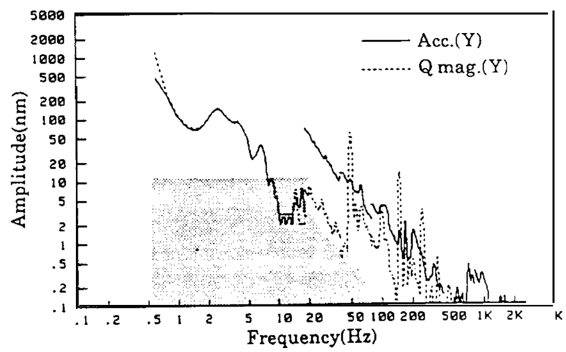

(d) Y direction of Q mag. and Acc.

Fig. 3.13 Displacement spectra in the operational state of cooling water in system A

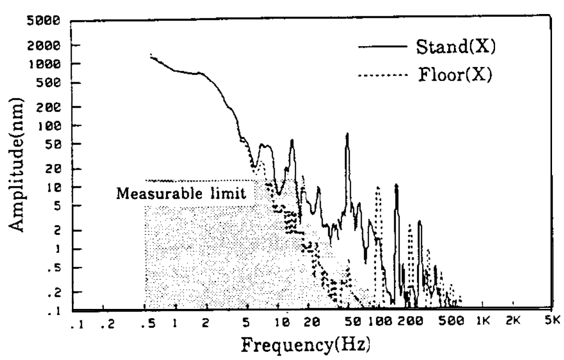

(a) X direction of Floor and Stand

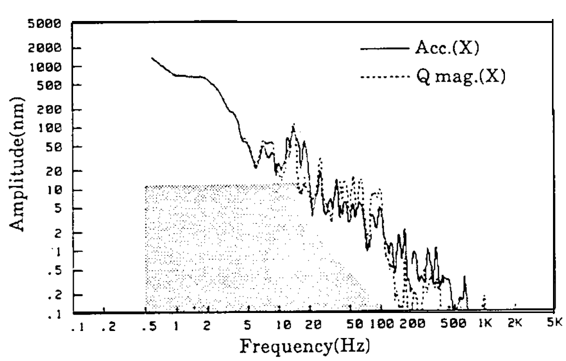

(b) X direction of Q mag. and Acc.

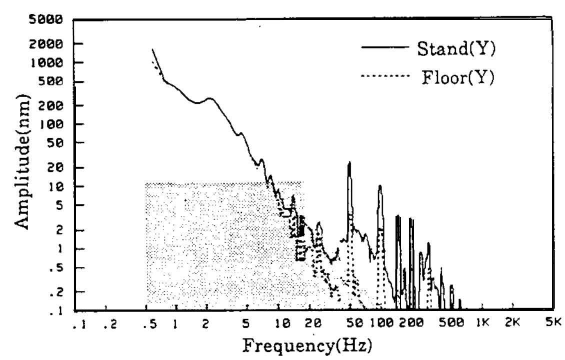

(c) Y direction of Floor and Stand

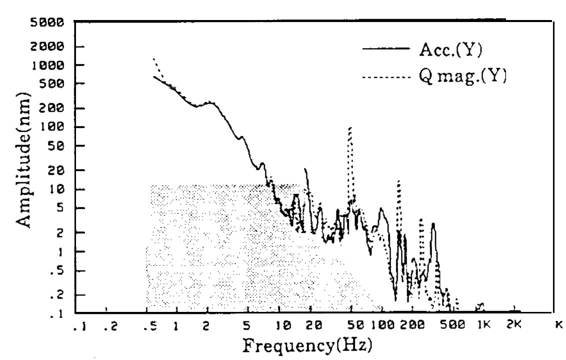

(d) Y direction of Q mag. and Acc.

Fig. 3.14 Displacement spectra in the operational state of cooling water in system B

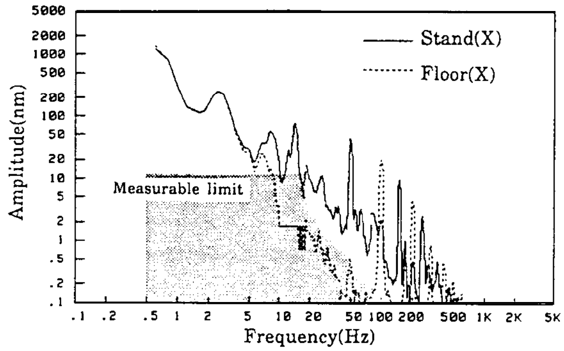

(a) X direction of Floor and Stand

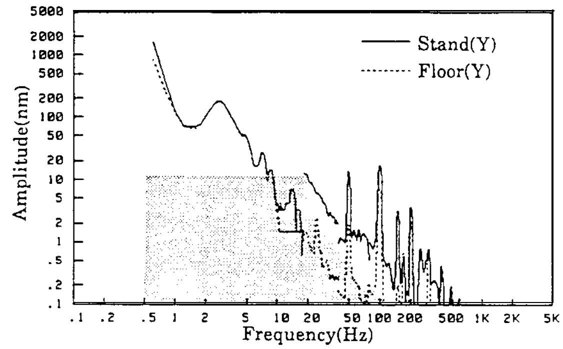

(c) Y direction of Floor and Stand

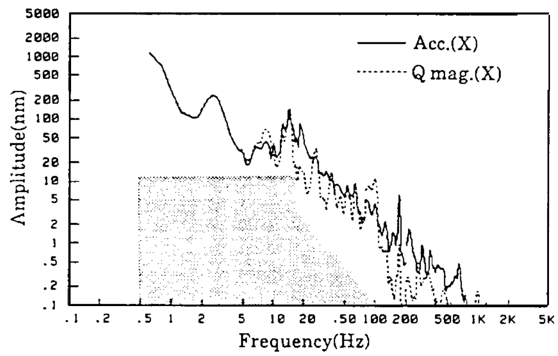

(b) X direction of Q mag. and Acc.

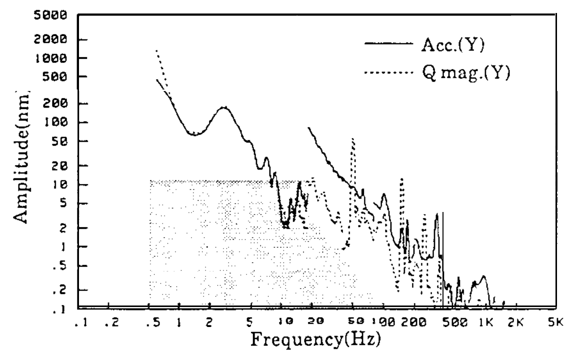

(d) Y direction of Q mag. and Acc.

Fig. 3.15 Displacement spectra in the operational state of cooling water in A + B + C

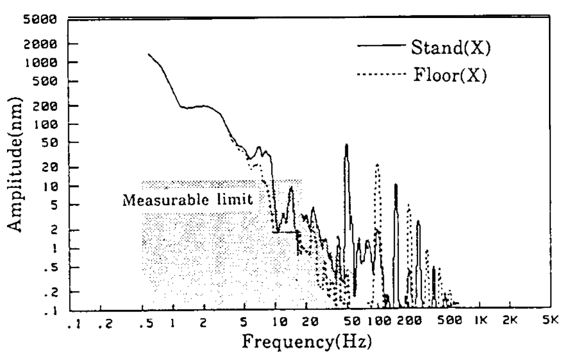

(a) X direction of Floor and Stand

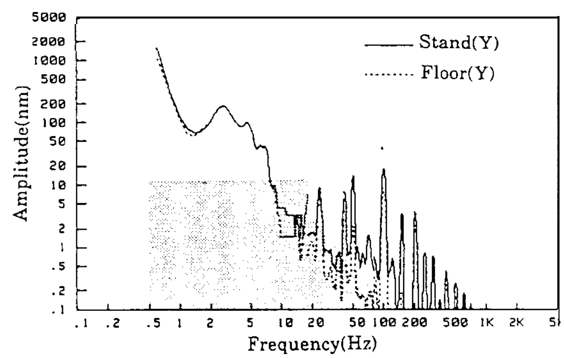

(c) Y direction of Floor and Stand

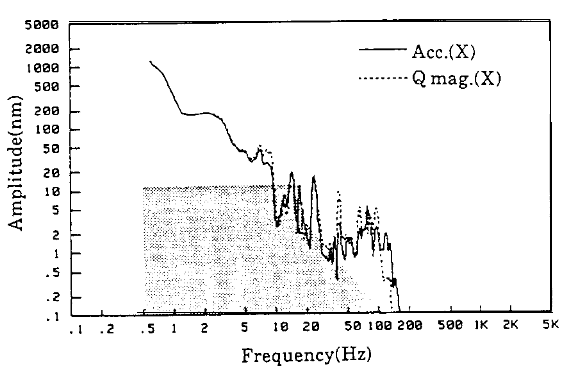

(b) X direction of Q mag. and Acc.

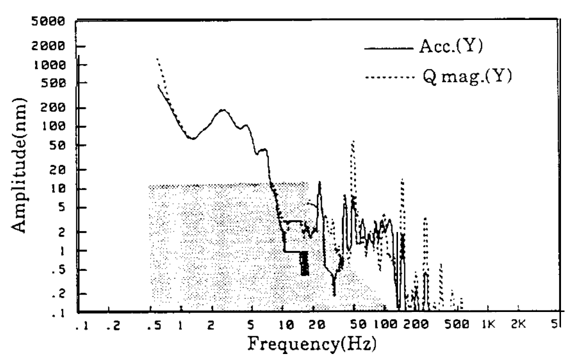

(d) Y direction of Q mag. and Acc.

Fig. 3.16 Displacement spectra when only the air cond. equipment is being operated